Article:
Fairbanks, S.D. orcid.org/0000-0002-5063-1367, Robertson, C.C., Keene, F.R. orcid.org/0000-0001-7759-0465 et al. (2 more authors) (2019) Structural investigation into the threading intercalation of a chiral dinuclear ruthenium(II) polypyridyl complex through a B-DNA oligonucleotide. Journal of the American Chemical Society, 141 (11). pp. 4644-4652. ISSN 0002-7863

https://doi.org/10.1021/jacs.8b12280

Structural investigation into the threading intercalation of a chiral dinuclear ruthenium (II) polypyridyl complex through a B-DNA oligonucleotide

Simon D. Fairbanks,[†‡] Craig C. Robertson,[†] F. Richard Keene,[§] Jim A. Thomas[†]* and Mike P. Williamson[‡]*

[†]Department of Chemistry, University of Sheffield, Brook Hill, Sheffield, S3 7HF, UK.

Email: james.thomas@sheffield.ac.uk; Fax: +44-(0)114-22-29436

[‡]Department of Molecular Biology and Biotechnology, University of Sheffield, Western Bank, Sheffield, S10 2TN, UK. Email: m.williamson@sheffield.ac.uk.

[§]Department of Chemistry, School of Physical Sciences, University of Adelaide, Adelaide, SA 5005, Australia.

KEYWORDS DNA; intercalation; chirality; chiral resolution; ruthenium; NMR structure; dynamics

ABSTRACT: Herein we report the separation of the three stereoisomers of the DNA light-switch compound $[\{Ru(bpy)_2\}_2(tpphz)]^{4+}$(tpphz = tetrapyrido[3,2-a:2',3'-c:3'',2''-h:2''',3'''-j]phenazine) by column chromatography and the characterization of each stereoisomer by x-ray crystallography. The interaction of these compounds with a DNA octanucleotide d(GCATATCG).d(CGATATGC) has been studied using NMR techniques. Selective deuteration of the bipyridyl rings was needed to provide sufficient spectral resolution to characterize structures. NMR-derived structures for these complexes show a threading intercalation binding mode with slow and chirality-dependent rates. This represents the first solution structure of an intercalated bis-ruthenium ligand. Intriguingly, we find that the binding site selectivity is dependent on the nature of the stereoisomer employed, with Λ Ru^{II} centers showing a better intercalation fit.

Introduction

Subcellular imaging of organelles and biomolecules such as DNA is not only of increasing importance in basic research and diagnostics, but also aids in understanding the dynamics of the DNA structure itself within cells. Most currently employed DNA-imaging probes require ultraviolet (UV) light, which can cause structural damage to DNA,[1] and also possess low water solubility, both factors affecting their application in live cell imaging. Recently, it has been demonstrated that DNA metallointercalators offer a promising range of photophysical properties to overcome these limitations.

Polypyridylruthenium coordination complexes such as $[Ru(bpy)_2(dppz)]^{2+}$ (bpy = 2,2'-bipyridine; dppz = dipyrido[3,2-a:2',3'-c] phenazine) are known to display a molecular 'light-switch' effect when reversibly binding to DNA.[2] In aqueous environments the expected Ru→dppz metal-to-ligand charge transfer (MLCT) luminescence is quenched due to interaction with the bulk solvent. As intercalation into DNA renders the ligand less solvent accessible, the MLCT emission is consequently "switched on". This property makes such complexes ideal candidates for the engineering of sensitive and structure-specific DNA probes.

With the aim of identifying systems with greater selectivity and increased binding affinities, more recent work has extended such studies to include oligonuclear complexes. In this context, the dinuclear Ru^{II} complex $[\{(Ru(bpy)_2\}_2(tpphz)]^{4+}$ (tpphz = tetrapyrido[3,2-a:2',3'-c:3'',2''-h:2''',3'''-j]phenazine) **(1)** (Figure 1) is of particular interest as we have previously shown that this complex binds to DNA quadruplex structures with a preference for the human telomere sequence (HTS) over duplex DNA.[3] Structural studies on the binding of **1** to HTS involving NMR and molecular dynamics showed that chirality plays an important role in this binding preference. It was found that only the Λ,Λ stereoisomer is capable of threading through the diagonal loop of antiparallel folded HTS to provide high affinity, whilst the Δ,Δ complexes actually prefer duplex over quadruplex DNA.[4]

Whilst these NMR structures provide insight into how this complex binds to quadruplex DNA, there are no definitive X-ray crystallographic or solution studies as to how **1** binds to B-DNA. There are two possibilities: intercalation or groove binding.

Work by Lincoln and Nordén has shown that related, but more extended, dinuclear ruthenium complexes can bind to duplexes through threading interactions, in which the bridging ligand is intercalated between the base pairs, with the bulky ruthenium centers localized in either groove. The intercalation process itself has a slow kinetic profile as a bulky ruthenium center needs to thread between the base pair stack, and so this process is associated with slow dissociation and association kinetics.[5]

By contrast, previous viscosity measurements have indicated that **1** does not spontaneously intercalate into duplex DNA,[6] and attempts to thread the complex into genomic calf thymus DNA (ct-DNA) by annealing were also unsuccessful. Therefore, despite the fact that the complex does show a light-switch effect, it was concluded that **1** binds to duplex DNA by groove binding rather than intercalating. This is consistent with a report by Lincoln *et al*. showing that, as the extended bridging ligands of their systems were shortened, threading of the complexes into ct-DNA was

inhibited,[7] until the shortest bridged complex only threaded into the more flexible poly-d(AT) DNA. However, in other studies, the same group has demonstrated that chirality of the threading moiety can have a significant impact on the kinetics and thermodynamics of binding events.[8,9]

Therefore, with the aim of developing a deeper structural understanding of how **1** interacts with DNA, we set out to separate the *rac* (Δ,Δ/Λ,Λ) and *meso* (Δ, Λ) diastereoisomers of the complex, resolve the former into its enantiomers, and investigate their individual interactions with the d(GCATATCG).d(CGATATGC) B-DNA oligonucleotide through high-field NMR.

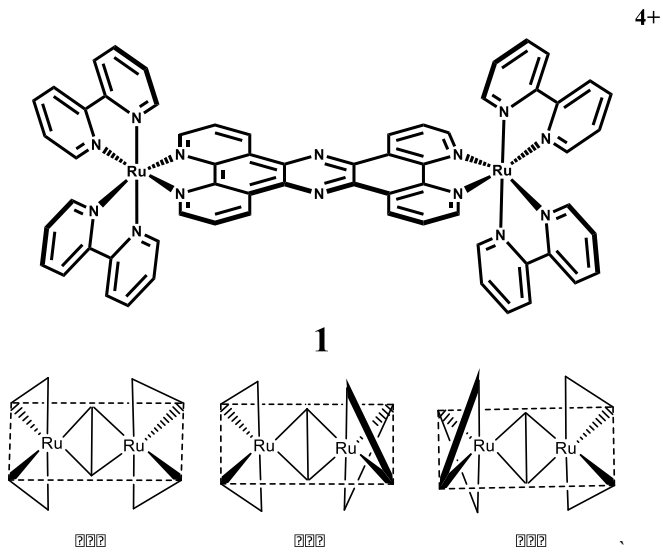

Figure 1. $[\{Ru(bpy)_2\}_2(tpphz)]^{4+}$ (bpy = 2,2"-bipyridine) (tpphz = tetrapyrido[3,2-a:2',3'-c:3'',2''-h:2''',3'''-j]phenazine) (**1**) and a representation of the stereoisomers (left to right) Λ,Δ; Λ,Λ and Δ,Δ.

Materials and Methods

All DNA oligonucleotides were bought from Eurogentec Biotechnology (Southampton), purified by HPLC-RP and freeze dried.

Metal complex synthesis. The $[Ru\{(bpy)_2\}_2(tpphz)](PF_6)_4$ was synthesized via literature methods and converted to its chloride salt using a Dowex anion-exchange resin.[11] ^{1}H NMR (800 MHz, D_2O) δ 10.03 (d, *J* = 7.8 Hz, 4H), 8.66 (d, *J* = 8.1 Hz, 4H), 8.63 (d, *J* = 8.1 Hz, 4H), 8.44 (d, *J* = 4.8 Hz, 4H), 8.18 (t, *J* = 7.8 Hz, 4H), 8.14 – 7.95 (m, 12H), 7.88 (d, *J* = 5.2 Hz, 4H), 7.51 (t, *J* = 6.3 Hz 4H), 7.30 (t, *J* = 6.3 Hz, 4H). MS; m/z (%): 303 (100) $[M^{4+}$-4Cl].

$[Ru\{(bpy\text{-}d_8)_2\}_2(tpphz)]Cl_4$ was synthesized using the same procedure starting with perdeuterated 2,2'-bipyridine-d_8. ^{1}H NMR (800 MHz, D_2O) δ 10.03 (d, *J* = 8.1 Hz, 4H), 8.45 (d, *J* = 5.4 Hz, 4H), 8.05 (dd, *J* = 8.1, 5.4 Hz, 4H). MS; m/z (%): 310.8 (100) $[M^{4+}$-4Cl].

Separation of stereoisomers. $[\{Ru(bpy)_2\}_2(tpphz)](PF_6)_4$ was converted into the chloride salt by stirring in an aqueous suspension of Dowex 1×8 chloride form overnight. The resin was removed by filtration and the filtrate was loaded onto a column system containing SP-Sephadex C25 with the flow controlled and circulated around the column by a peristaltic pump with a flow rate of 0.75 ml min^{-1}. The addition of an eluent solution of 0.15 mM sodium octanoate caused a band to progress down the column and the system was set up to recycle. After several passes of the column there was clear separation into two red bands. The first (*meso*; Λ,Δ) and second (*rac*; Δ,Δ/Λ,Λ) fractions were collected and extracted with the addition of NH_4PF_6 into dichloromethane and dried using $MgSO_4$. The organic layer was filtered and the solvent removed under reduced pressure to give the PF_6^- salts which were converted by metathesis to the chloride salts by dissolution in acetone and precipitation using tetra-*n*-butylammonium chloride.

The racemic band was then reloaded onto the column with the same method above and eluted using a solution of 0.05 M sodium dibenzoyl-L-tartrate. Only one passage of the column was needed to see complete separation with the Δ,Δ eluted first and the Λ,Λ second. The two fractions were collected and extracted with the addition of NH_4PF_6 into dichloromethane and dried using $MgSO_4$. The organic layer was filtered and the solvent removed under reduced pressure to give the PF_6^- salts which were converted to the chloride salts by dissolution in acetone and precipitation using tetra-*n*-butylammonium chloride.

Simulated annealing. Molecular dynamics refinement of the NMR structure was carried out using CNS.[12,13] Structure files for the ruthenium complexes were created using xplo2d software using coordinates obtained from a crystal structure.[14] Coordinates for the B-DNA were generated using the DNA sequence-to-structure web tool using conformational parameters taken from fiber-diffraction studies.[15] Structure files for the DNA were generated using the generate_easy.inp function within CNS. Simulated annealing was performed using the model_anneal.inp function. To maintain the duplex B-DNA structure, the planarity and H-bonds of the base pairing and also the dihedral angles involved in C2' endo sugar puckering were restrained. The backbone dihedral angle restraints measured from the starting structure (α = -46.8°, β = -146.1°, γ = 36.4°, δ = 156.4°, ε = 155°, ζ = -97.8°) were given a range of ± 30° for bases adjacent to the intercalation site and ± 5° for other residues.[16] Experimental NOEs were added as structural restraints and classified as strong (1.8 - 3 Å), medium (1.8 - 4 Å) and weak (1.8 - 5 Å) based on the cross peak intensity compared to known DNA inter-proton distances.[17] Complex calculation was started with well-separated ligand and duplex structures and an energy minimization was performed. This was followed by a high-temperature annealing stage heating up to 1000 K in 1000 steps. During the 15 picosecond high temperature dynamics phase the van der Waals energy term was reduced to 0.1 to facilitate threading. This was followed by a 15 picosecond cooling phase over 1000 steps in which the van der Waals energy term was scaled back up to one, followed by a Powell minimization to give the final structure.

Results and Discussion

Synthesis and Characterization. The chromatographic separation of **1** on SP-Sephadex C25 cation exchange resin into its three stereoisomers was performed using a method developed by Keene et al,[18] in which separation of diastereoisomers is achieved through the differential association of an eluent anion with the cationic complex. In agreement with previous studies the *meso* compound Λ,Δ-**1** eluted first using the aliphatic octanoate anion.

The racemic mixture of Δ,Δ-**1** and Λ,Λ-**1** was subsequently separated by the use of a chiral eluent, sodium dibenzoyl-L-tartrate, which first eluted the Δ,Δ-**1** cation. The separation of three isomers was confirmed by circular dichroism (CD) measurements (Figure 2), and X-ray crystallography (Figure 3). Interestingly, there was no difference in the NMR spectra of the Δ,Δ, Λ,Λ and Λ,Δ forms, as has been reported for shorter-bridged ruthenium dimers.[19]

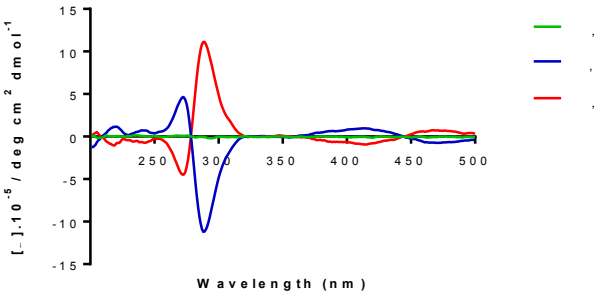

Figure 2. The normalized CD spectra of Λ,Λ, Δ,Δ and Λ,Δ-**1** as a 15 μM solution in H_2O, recorded on a Jasco J-810 spectropolarimeter at 25 °C, scanning at 100 nm/min from 500-200 nm.

X-ray crystallography. It was previously reported that crystals of **1** were grown from an unresolved mixture of stereoisomers as its nitrate salt and resulted in a structure which solely contained co-crystallized Δ,Δ and Λ,Λ forms.[21] It was speculated that this occurred because Λ,Δ-**1** was more soluble than the other two forms. Therefore, following our successful separation of all three stereoisomers, we set out to obtain individual structures of Λ,Λ -**1,** Δ,Δ-**1** and Λ,Δ-**1**. To our knowledge, this represents the first example of a crystallographic study on all three individual stereoisomers of a dinuclear ruthenium polypyridyl complex.[22]

Crystals of Λ,Δ-**1** suitable for X-ray structure determination were grown by the slow diffusion of acetone into a methanolic solution of its chloride salt. The asymmetric unit consists of half of the molecule along the bridging tpphz moiety, such that applying inversion symmetry generated the other half of the molecule in the full unit cell. As expected, the extended polyaromatic tpphz bridging ligand is almost completely planar. The ruthenium-nitrogen bond lengths are 2.045-2.068 Å and bite angles are 78.58-79.2°. In contrast to the previously reported structure, in which dinuclear cations are orthogonally stacked over each other, the cations in the Λ,Δ-**1**Cl_4 structure are arranged in the offset coplanar stack to form layers with the chloride counter ions in channels between them (Figure 3a). Thermal ellipsoid plots and further crystallographic data are shown in Supplementary Information (SI 1).

Crystals of Λ,Λ-**1** and Δ,Δ-**1** suitable for X-ray structure determination were grown (SI 1). Interestingly, packing within the crystal structures of the individual enantiomers is very different from the previously reported structure that contained both forms together. However, the structures of the isolated enantiomers are almost perfect mirror images of each other with an inversion of one yielding the structure of the other (Figure 3b,3c). The Λ,Λ-**1** ruthenium-nitrogen bond lengths are 2.035-2.093 Å and bite angles 78.36-79.91°. Δ,Δ-**1** ruthenium-nitrogen bond lengths are 2.038-2.113 Å and bite angles 77.89-80.12°. Interestingly the structure obtained from the crystals grown from pre-resolved complexes shows a co-planar stacking arrangement similar to that seen in the Λ,Δ-**1** structure with a greater separation caused by the larger PF_6^- anions.

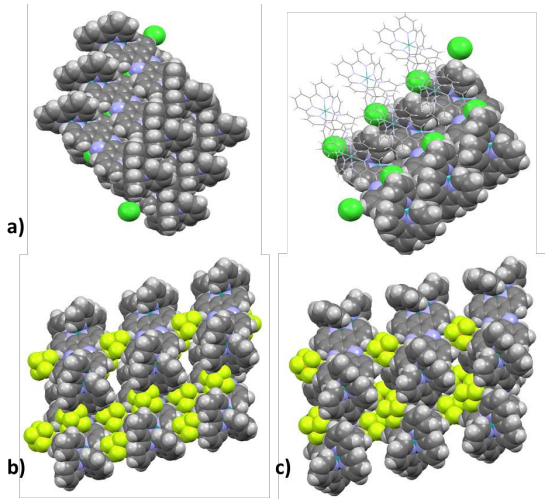

Figure 3. Crystallographic structures of a) Λ,Δ-**1** b) Λ,Λ-**1** and c) Δ,Δ-**1** with Cl^- (green) and PF_6^- (yellow) counter ions outlined.

With detailed structural data for all three stereoisomers of **1** to hand, we then set out to explore their interactions with a specific duplex DNA sequence.

Duplex Stability Studies. Studies were carried out using a non self-complementary DNA octanucleotide sequence d(GCATATCG).d(CGATATGC), designed to be short but contain a range of different dinucleotide sequences, with dG.dC base pairs at the ends to prevent fraying. Concentrations of 2 mM were employed to ensure the DNA was in a stable duplex form, as at lower concentrations the DNA began to melt into single strands.

Optical spectroscopy studies with DNA. Although Λ,Δ-**1** has no CD signal, on addition of the *meso* Λ,Δ-**1** to the oligonucleotide d(GCATATCG).d(CGATATGC), a positive induced CD signal is seen at λ_{max} 465 nm (SI 2), consistent with the formation of an intercalated (threaded) complex.[8,20] Whilst Λ,Λ-**1** and Δ,Δ-**1** are both intrinsically CD-active, and therefore the induced CD (iCD) signal is less clean, it is clear that their interaction with the sequence also results in an enhanced signal due an additional iCD component.

As **1** is emissive in aqueous solutions when bound to DNA, we also investigated the lifetimes of the three stereoisomers when interacting with d(GCATATCG).d(CGATATGC). Like many of their analogs, the duplex bound complexes all display biexponential decay (SI 3) but there are some some differences between Δ,Δ-**1** and the other two stereoisomers. The data for Λ,Δ-**1** and Λ,Λ-**1** are quite similar, with both showing a ~70% contribution from a long lived major component of τ =164.4 and τ =147.4 ns respectively. Within experimental error, a shorter lifetime component is almost identical for the two stereoisomers (Λ,Δ-**1** τ = 99.4 ± 5.5 ns; 30%); Λ,Λ-**1** τ = 90.5 ± 6.5 ns; 31%). The ΔΔ-**1** stereoisomer displays a significantly larger contribution from a longer lived component (τ = 175.6 ± 1.4 ns; 95%) and the second lifetime is significantly shorter than for the other two stereoisomers (τ = 72.0 ± 10.7 ns; 5%). These data suggest that the interaction of Δ,Δ-**1** with duplex DNA is somewhat different to that of the other stereoisomers.

NMR Studies. ^{1}H NMR spectra of the free DNA duplex were assigned unambiguously using standard methods,[23] and indicate a

standard B-DNA conformation (SI 4).[24] Binding studies containing metal complexes were performed up to a ligand:duplex ratio of 0.5:1, as higher concentrations than this led to broadened NMR spectra and DNA precipitation. Free metal complex resonances were also assigned (SI 5), aided by an inter-ligand NOE between bipyridine and tpphz.

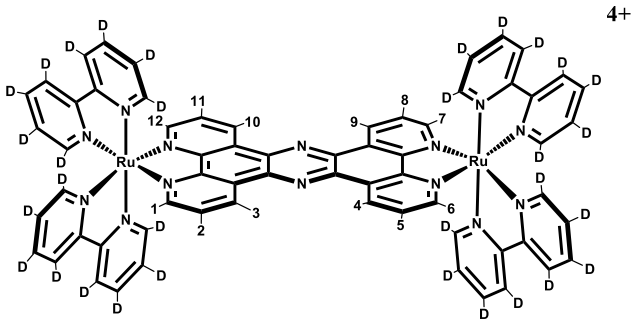

Figure 4. $[\{Ru(bpy\text{-}d_8)_2\}_2(tpphz)]^{4+}$ (bpy = 2,2”-bipyridine-d_8 and tpphz = tetrapyrido[3,2-a:’,3’-c:3’’,2’’-h:2’’,3’’’-j]phenazine). The proton labelling scheme of the complex is indicated in the structure.

Preliminary ^{1}H-NMR binding study. Titration of unresolved **1** into the DNA solution showed the complex to be in a slow-exchange regime, implying that the dissociation rate is slow on the NMR timescale. For the free metal complex , the sets of pseudo-symmetry related protons (ie the tpphz proton sets [1, 6, 7, 12], [2, 5, 8, 11] and [3, 4, 9, 10], see Figure 4, as well as many of the bpy protons) have identical chemical shifts.

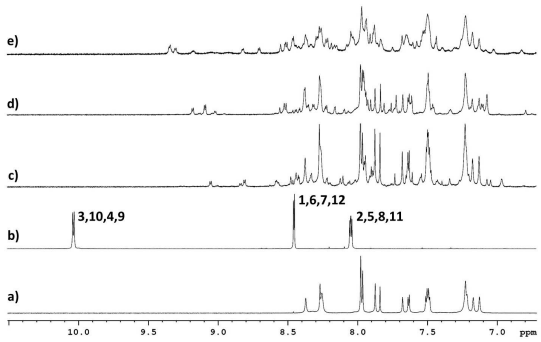

Figure 5. The aromatic region of 1D ^{1}H-NMR spectra showing the addition of 1 mM $[\{Ru(bpy\text{-}d_8)_2\}_2(tpphz)]^{4+}$ to a 2 mM solution of DNA oligonucleotide d(GCATATCG).d(CGATATGC) in D_2O. a) DNA alone. b) $[\{Ru(bpy\text{-}d_8)_2\}_2(tpphz)]^{4+}$. Sets of equivalent tpphz protons are indicated. c) DNA + d-Λ,Δ-**1.** d) DNA + d-Λ,Λ-**1.** e) DNA + d-Δ,Δ-**1**.

However in the DNA complex each group of protons gives at least four different bound signals, for each stereoisomer and bound conformer. The NMR spectrum of the bound ligand is therefore very complex and is unassignable. Although binding of each of the separated stereoisomers produced more assignable spectra, the non-equivalence of bipyridyl protons resulted in an overcrowded aromatic region. Therefore, bpy-d_8 was employed to simplify the spectra by removing bpy ligand proton resonances to leave only the tpphz protons as NMR active (Figure 4).[25] In these conditions even a cursory inspection of the 1D NMR spectra reveals large upfield shifts for tpphz protons for all stereoisomers (Figure 5).

Addition of d-Λ,Λ-1 to d(GCATATCG).d(CGATATGC). Upon titration of deuterated Λ,Λ-**1** (d-Λ,Λ-**1**) into the DNA duplex, two distinct sets of resonances for the bound complex became apparent with a ratio of 2:1, indicating the existence of two binding sites or modes for this complex. Both of these bound forms were in slow exchange with the free DNA and had well-dispersed peaks, permitting unambiguous assignment (SI 6). The major bound form, denoted d-Λ,Λ-**1A**, showed large changes in DNA chemical shifts at the central (T4,A13)|(A5,T12) base step as a result of the ring current from the aromatic complex (Figure 6). This preference for (T4,A13)|(A5,T12) is likely to be due to the lower stability and higher flexibility of AT-rich tracts as observed with similar compounds in previous studies.[26] Notably, very large chemical shift changes (Δδ = -1.61 ppm) were seen for the adjacent thymidine methyl protons located in the major groove of the DNA. Sizeable shifts were also seen for the sugar protons located in the minor groove indicative of an intercalation binding mode. By contrast, the minor bound species (d-Λ,Λ-**1B**) displayed large changes in chemical shift at the (C2,G15)|(A3,T14) binding site with almost zero perturbation to chemical shift at the other end of the duplex (Figure 6). The largest change in chemical shift (-2.17 ppm) is assigned to the thymidine methyl proton in the major groove along with other significant perturbations for chemical shifts of protons located in the minor groove. We note that the two intercalation sites observed for d-Λ,Λ-**1** are C2|A3 and T4|A5 with no detectable binding anywhere else, suggesting a preference for a pyrimidine|A.T|purine sequence. It is of interest that these two dinucleotide sequences have the largest roll and almost the smallest twist and greatest flexibility of all dinucleotide sequences,[27] further highlighting the importance of the local structure and flexibility of the intercalation site. d-Λ,Λ-**1** resonances were shifted upfield upon binding the DNA. The largest upfield shifts to the central protons (3,4,9,10) are also consistent with an intercalation binding mode with the central protons more aligned on top of the base stack (SI 7) .[25]

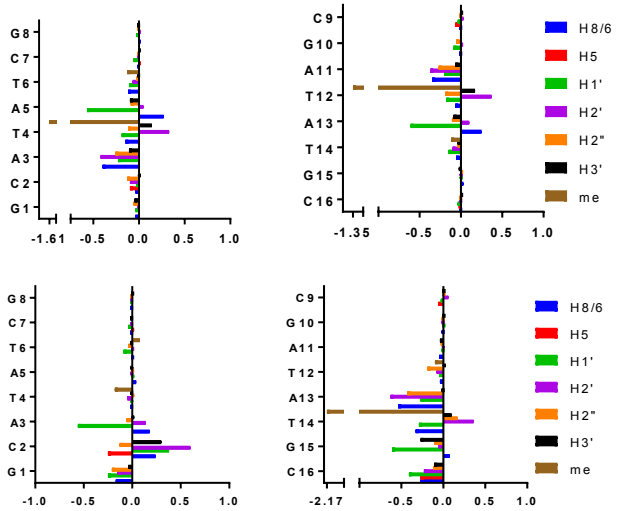

Figure 6. Chemical shift perturbations in ppm of duplex $d(G_1C_2A_3T_4A_5T_6C_7G_8).d(C_9G_{10}A_{11}T_{12}A_{13}T_{14}G_{15}C_{16})$ for the major and minor bound forms seen upon addition of half an equivalent of d-Λ,Λ-**1**. d-Λ,Λ-**1A** (top); d-Λ,Λ-**1B** (bottom).

NOE studies with d-Λ,Λ-1. For the (d-Λ,Λ-**1A**)-DNA complex, 30 intermolecular NOEs were assignable from the DNA to the tpphz protons (SI 8). These NOEs localize at the (T4,A13)|(A5,T12) binding site and extend into both the major

and minor grooves and from both ends of the tpphz ligands. Comparison with the non-deuterated sample shows that few NOEs were seen from the bipyridine ancillary ligands with only two to the thymine methyl protons in the major groove. Interestingly, on inspection of the intramolecular DNA NOEs, the binding of the metal complex causes a break in the internucleotide 5'-3' NOE walk at (T4,A13)|(A5,T12). This indicates that the binding of the complex causes the separation of T4|A5 and T12|A13 at this site. It is also possible to use internucleotide NOEs from d-Λ,Λ-**1A** to complete the sequential assignment (Figure 7). This is a very strong indication of intercalation, with d-Λ,Λ-**1** residing in between the base pairs.

The minor bound species, d-Λ,Λ-**1B**, showed 24 assignable intermolecular NOEs (SI 8). The NOEs reside at one end of the DNA duplex with connectivities to C2A3/T14G15 with a similar pattern to that seen for the d-Λ,Λ-**1A** species extending into both grooves of the DNA. In a similar way to the major species NOE walk, a break occurs at C2|A3 and T14|G15 with the sequential assignment being completed through close contacts to the d-Λ,Λ-**1B** protons.

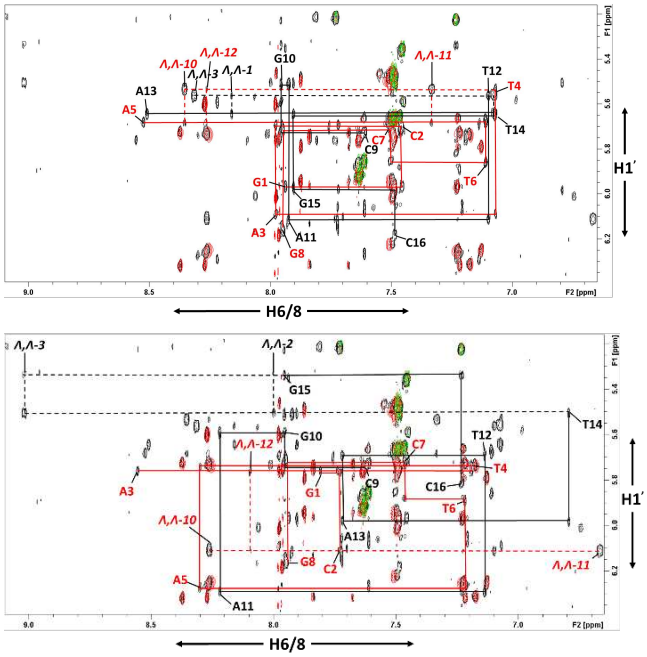

Figure 7. Expansion of the H1'-H6/8 region of the NOESY spectrum of a d($G_1C_2A_3T_4A_5T_6C_7G_8$).d($C_9G_{10}A_{11}T_{12}A_{13}T_{14}G_{15}C_{16}$) DNA/d-Λ,Λ-**1** complex. The solid lines show the DNA NOE walk and dashed lines show NOE connectivities between d-Λ,Λ-**1A** (top), d-Λ,Λ-**1B** (bottom) and the DNA 1' protons. The overlaid NMR spectra show the NOESY spectra of 2mM DNA (red); 2mM DNA, 1mM d-Λ,Λ-**1** (black); and the COSY spectrum of 2mM DNA, 1mM d-Λ,Λ-**1** (green).

Addition of d-Λ,Δ-1 to d(GCATATCG).d(CGATATGC). Addition of d-Λ,Δ-**1** to DNA in a 1:2 ligand:duplex ratio also resulted in two sets of DNA resonances in slow exchange, highlighting two binding modes in a similar ratio as observed for the d-Λ,Λ-**1** species. Although both binding events take place at the same (T4,A13)|(A5,T12) site, only the major conformer, d-Λ,Δ-**1A** was unambiguously assignable due to insufficient spectral dispersion of the minor species (d-Λ,Δ-**1B**). The changes in chemical shift for d-Λ,Δ-**1A** display a profile comparable to that of d-Λ,Λ-**1A**, implying a structurally similar intercalated structure (Figure 8). d-Λ,Δ-**1A** resonances were shifted upfield upon binding to the DNA, with the largest shifts to the central protons (3,4,9,10), consistent with an intercalative binding mode (SI 7).[25]

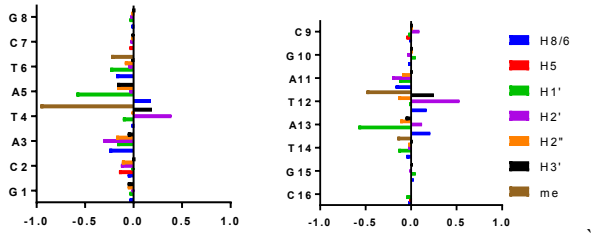

Figure 8. Chemical shift perturbations in ppm of duplex d($G_1C_2A_3T_4A_5T_6C_7G_8$).d($C_9G_{10}A_{11}T_{12}A_{13}T_{14}G_{15}C_{16}$) upon addition of half an equivalent of d-Λ,Δ-**1A**.

The thymidine methyl protons of d-Λ,Δ-**1B** are identified by H6/8-TMe crosspeaks in the TOCSY spectrum. Two of these show very large upfield chemical shift changes upon binding (~ 1.6 ppm) (SI 9), implying intercalation at a site adjacent to two thymidine methyls with a similar chemical shift perturbation to that of d-Λ,Λ-**1A**. The thymidine methyls reside in the major groove of the DNA, therefore the similar chemical shift strongly implies a similar major groove conformation with the Λ Ru^{II} center residing in the major groove.

Of the assignable intermolecular NOEs from the DNA to the tpphz protons for d-Λ,Δ-**1A**, 23 out of 24 were also present in d-Λ,Λ-**1A**. This implies a similar binding regime for both complexes: intercalation at the central (T4,A13)|(A5,T12) base step with NOEs extending into both grooves of the DNA (SI 8).

Similarly to d-Λ,Λ-**1A** the sequential internucleotide NOE assignment is disrupted at the binding site with completion of the "walk" provided via intermolecular NOEs to d-Λ,Δ-**1A**, indicating that the ligand is stacking between the base pairs of the DNA and increasing the internucleotide separation at this site (Figure 9).

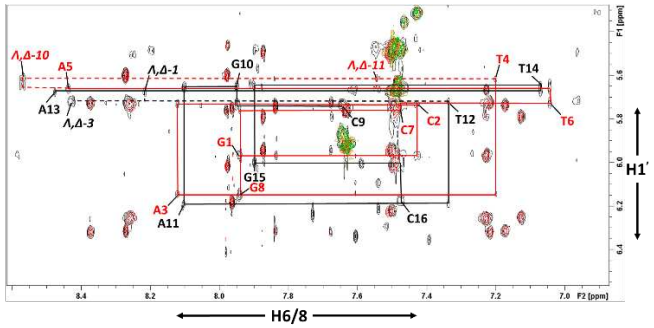

Figure 9. Expansion of the H1'-H6/8 region of NOESY and COSY spectra of a d($G_1C_2A_3T_4A_5T_6C_7G_8$).d($C_9G_{10}A_{11}T_{12}A_{13}T_{14}G_{15}C_{16}$) DNA/Λ,Δ-1 complex. The solid lines show the DNA 1'-H6/8 internucleotide NOE walk, and dashed lines show NOE connectivities between d-Λ,Δ-**1A** and the DNA 1' protons. The overlaid NMR spectra show the NOESY spectra of 2mM DNA (red); 2mM DNA + 1mM d-Λ,Δ-**1** (black); and the COSY spectrum of 2mM DNA + 1mM d-Λ,Δ-**1** (green).

Addition of d-Δ,Δ-1 to d(GCATATCG).d(CGATATGC). Upon addition of d-Δ,Δ-**1** to the DNA duplex, two sets of broadened signals are observed in intermediate to slow exchange, with pairs of exchange peaks in the NOESY spectrum. The clearest set of exchange peaks can be seen for the thymidine methyl (TMe) signals as they are upfield in an uncrowded region of the spectrum (Figure 10). Whilst the spectrum is generally unassignable due to spectral overcrowding from the multiple exchange peaks, the TMe signals can be assigned from TOCSY and COSY spectra. Intermolecular NOEs between TMe protons and d-Δ,Δ exist in one of the two conformations, similar to those seen for the Λ,Δ and Λ,Λ stereoisomers. There are also large chemical shift differences between the signals in the two bound conformations with one set of resonances shifted upfield by 0.6 ppm. The TMe protons are located in the major groove of the DNA duplex. Thus, one of the two conformations has highly shifted TMe signals and NOE close contacts to d-Δ,Δ-**1** indicating a threaded state. The other conformation has comparatively small chemical shift changes for the TMe protons. All the other complexes presented in this work contain at least one TMe signal shifted extensively due to ring current shifts from an adjacent intercalated ligand. The small shift changes suggest a different mode of binding of d-Δ,Δ-**1** for this second conformer, most likely in the minor groove of the DNA. It has been previously reported that binuclear ruthenium complexes can associate with DNA within its minor groove and this becomes the starting point for the intercalative threading at AT residues.[28] The dynamic exchange behavior observed in our experiments suggests the threading process is occurring with d-Δ,Δ-**1** translating from the minor groove through to the threaded state.

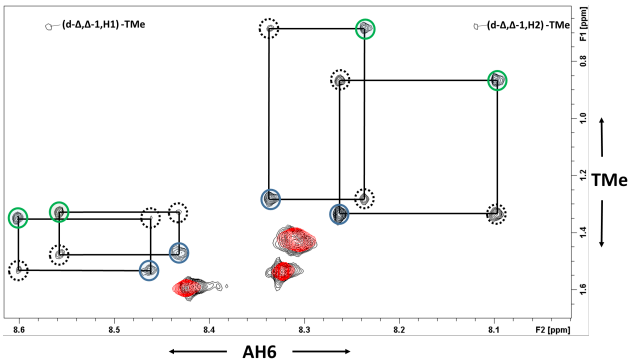

Figure 10. Expansion of NOESY spectra showing the AH6-TMe internucleotide connectivities of a solution containing 2 mM d(GCATATCG).d(CGATATGC) and 1 mM d-Δ,Δ-**1** in D_2O (black). The free DNA spectrum is overlaid for comparison (red). The circles outline AH6-TMe internucleotide couplings. Green circles: d-Δ,Δ-**1** threaded conformation. Blue circles: d-Δ,Δ-**1** minor groove conformation. Dashed circles: exchange peaks.

The exchange cross peak intensities from dynamic EXSY experiments at different mixing times and temperatures can be used to determine activation energy parameters (SI 10).[29] Using an Arrhenius analysis, the activation energy (E_a) for the transition was found to be 116 kJmol^{-1}. Subsequent use of the Eyring equation led to enthalpy ($\Delta H^{\ddagger}$) and entropy ($\Delta S^{\ddagger}$) estimates of 114.1 kJmol^{-1} and 140.3 Jmol^{-1} K^{-1} respectively, values that are comparable to those obtained in previous studies. Specifically, in work on their more extended threading complex, but which incorporates the same $Ru^{II}(bpy)_2$ moieties, the Lincoln group reported that the Λ,Λ stereoisomer threads through poly-d(AT) DNA with an activation energy of 132 kJmol^{-1}.[26] The lower activation energy for threading of d-Δ,Δ-**1** is reflected in the faster exchange kinetics seen here.

It is significant that the free energies of the minor groove-bound and intercalated complexes of d-Δ,Δ-**1** are very similar, whereas for d-Λ,Λ-**1** and d-Λ,Δ-**1** there is a strong preference for an intercalated structure. Further, the exchange rate for reversible intercalation of d-Δ,Δ-**1** is faster than for the other two stereoisomers, implying that the explanation for this difference lies in an energetically less favorable intercalated structure, in other words that two Δ units fit less well into the DNA groove when intercalated than do Λ units. Intriguingly, this contrasts with structural studies on the enantiomers of mononuclear $[Ru(bpy)_2(dppz)]^{2+}$ which have indicated that the Δ form is a better fit to duplex DNA.[30-32]

^{31}P NMR

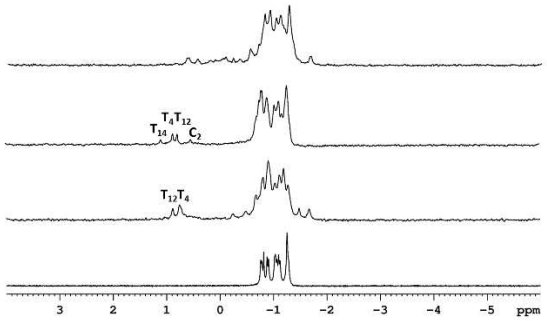

Figure 11. ^{31}P NMR spectra of $d(G_1C_2A_3T_4A_5T_6C_7G_8).d(C_9G_{10}A_{11}T_{12}A_{13}T_{14}G_{15}C_{16})$ $[\{Ru(bpy\text{-}d_8)_2\}_2(tpphz)]^{4+}$ with assignment of phosphorus atoms indicated. Phosphorus signals are labeled by the nucleotide that is attached by its 3' oxygen, so for example T_4 means the phosphate between T4 and A5. From bottom to top: free DNA (2mM), d-Λ,Δ-**1**/DNA (0.5:1), d-Λ,Λ-**1**/DNA (0.5:1) and d-Δ,Δ-**1**/DNA (0.5:1).

^{31}P NMR experiments provide further insight. Backbone phosphates were assigned using ^{31}P-^{1}H COSY experiments (SI 11). Phosphorus chemical shifts are sensitive to changes in backbone torsional angles. In particular, intercalation generally results in a downfield shift at the intercalation site.[5,33] The large downfield change in chemical shift for binding of the d-Λ,Λ-**1** and d-Λ,Δ-**1** stereoisomers (1.9 ppm, Figure 11) is indicative of intercalation affecting the backbone phosphates at the binding site, and confirms intercalation at the 4|5 and 2|3 steps as discussed above.

Interestingly the phosphates that are shifted downfield in the d-Λ,Λ-**1** spectra are T12,T4 and C2,T14 which correspond to d-Λ,Λ-**1A** and d-Λ,Λ-**1B** respectively. The shifted phosphorus nuclei in the Λ,Δ-**1** spectrum are T12,T4. Assignment of the d-Δ,Δ-**1** phosphorus spectra was not possible due to the exchange behavior although downfield shifted peaks suggest that an intercalated ligand is one of the bound conformations. All the data are therefore consistent with intercalation at the central (T4,A13)|(A5,T12) base step for d-Λ,Λ-**1A**, d-Λ,Δ-**1** and one of the d-Δ,Δ-**1** complexes, and at (C2,G15)|(A3,T14) for d-Λ,Λ-**1B**.

Simulated annealing models. Restrained molecular dynamics calculations were performed on the DNA duplex with Λ,Λ-**1A**, Λ,Λ-**1B** and Λ,Δ-**1** using experimentally derived NOEs (SI 8). For Λ,Λ-**1A**, the calculation produced a structure in which the ligand is intercalated at the central (T4,A13)|(A5,T12) base step,

as expected from the results presented above (Figure 12a). The structure had no NOE violations or unusually close van der Waals contacts. The Λ,Λ-**1B** simulated annealing calculation confirmed intercalation at the $C_2|A_3$ site with no NOE violations (Figure 12b). Restrained MD carried out on the Λ,Δ-**1**/DNA complex yielded two energy-minimised structures from the same NOE restraints from the tpphz ligand (Figure 12c). The two structures have the Λ and Δ Ru^{II} centers interchanged. The existence of these two structures is concordant with the NMR spectra showing two bound species. All of the structures show the complex more deeply inserted into the minor groove with the ruthenium center protruding out of the major groove.

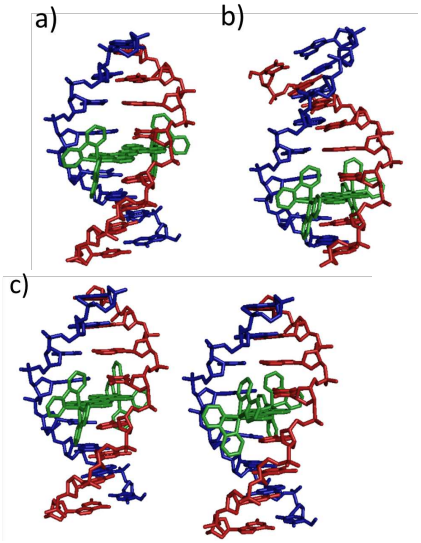

Figure 12. Resultant structures of restrained molecular dynamics calculations of a) Λ,Λ-**1A** b) Λ,Λ-**1B** and c) the two possible orientations of Λ,Δ.

The models show that the alignment of the bipyridyl units relative to the duplex in each chiral center plays a large role in the binding event. The twist of the bipyridyl ligands of a Δ Ru^{II} chiral center runs perpendicular to that of the grooves, whereas in a Λ Ru^{II} center they are aligned parallel to the grooves, giving a better fit (SI 12). This means that the bipyridyl protons in the Δ Ru^{II} point in towards the proximal DNA strand causing an unfavourable steric interaction. The most stable threaded complex is the Λ,Λ-1 which binds at the two most accessible sites (T4,A13)|(A5,T12) and (C2,G15)|(A3,T14). In Λ,Δ-**1**, a Λ chiral center compensates for the unfavourable steric interactions of a Δ center (Figure 13). This means it can still form a very stable threaded complex, although only at the most accessible (T4,A13)|(A5,T12) binding site. Conversely, the presence of two Δ centers in Δ,Δ-**1** results in a less stable threaded species which exhibits a stability that is comparable to that of the groove bound form, thus giving the observed population distribution.

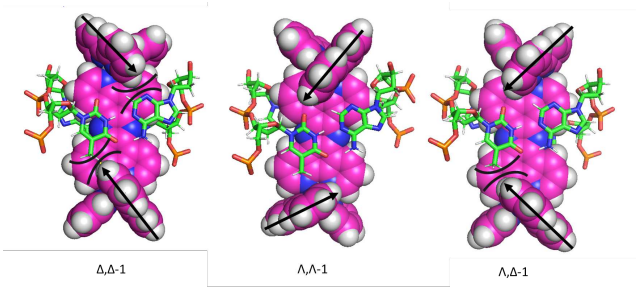

Figure 13. Views down the helical axis at the (T4,A13)|(A5,T12) binding site of the three stereoisomers of **1** bound to d(GCATATCG).(CGATATGC). Λ,Δ-**1** and Λ,Λ-**1** structures are produced from simulated annealing and Δ,Δ-**1** is a result of manually docking Δ,Δ-**1** into the Λ,Δ-**1** model. The arrows indicate the orientations of the bipyridyl ancillary ligands and the curves represent unfavorable steric clashes.

Discussion

Although **1** interacts with ct-DNA entirely through groove binding,[6] these studies indicate that **1** intercalates into an 8-mer oligonucleotide fragment through a threading interaction. As discussed above, it has been shown that for dinuclear ruthenium complexes linked by a bridging ligand, the length and rigidity of the bridge plays an important role in the selectivity and kinetics of threading. Shorter and more rigid bridges cannot thread into calf thymus DNA but threading through more flexible sequences such as poly-d(AT) DNA can still occur.[7,26] It has been suggested that as the bridging moieties become shorter it becomes progressively less favorable to have a Δ ruthenium center in the major groove.[20] The tpphz bridging moiety in **1** is far shorter and more rigid than previously studied threading complexes, where the curvature of the molecule matches the pitch of the DNA.[28] This means that in the groove-bound state of **1,** unfavourable steric clashes from a Λ-configured metal center to the right-handed DNA duplex would be increased thus favoring an intercalated form. It is also notable that a Δ-configured metal center forms unfavorable steric clashes when intercalated, with Δ,Δ-**1** being less stable in the threaded form than the other two stereoisomers. The Δ,Δ-**1** complex also shows rather faster kinetics than the Λ,Λ-**1** and Λ,Δ-**1** forms, with exchange occurring on the NMR timescale suggesting that the other two isomers are kinetically locked into the threaded mode as well as being thermodynamically more favored in the threaded form.

Slow kinetics is typical of threading intercalation as the bulky ruthenium centers need to pass through the duplex in order to dissociate. This is reflected in the Λ,Λ-**1** and Λ,Δ-**1** isomers. However, the proposed initial groove-bound state is not observed in this study for these stereoisomers. The DNA oligonucleotide sequence used in this study is of low stability and is mostly single-stranded at lower concentrations. It is proposed that the nucleotide sequence can thus form a lowly-populated single-stranded state which can re-fold around **1** and reach equilibrium before any NMR experiments are carried out. Therefore, the conformations observed are able to reach their most thermodynamically stable forms. The Δ,Δ-**1** isomer must be intercalating by creation of a transient opened or flipped-out state, into which the Δ,Δ-**1** isomer threads. The other two isomers intercalate more slowly. In other words, the transition state for intercalation of the Δ,Δ-**1** isomer must be significantly lower than that for the other isomers, this presumably being due to a steric match between the Δ,Δ-**1** isomer and the gap in a transiently open duplex. In turn, this implies that it should be possible to control

the intercalation rate by modifying the ruthenium ancillary ligands.

Conclusions

Our results show that the three stereoisomers of DNA binding compound $[\{Ru(bpy)_2\}_2(tpphz)]^{4+}$ all bind differently to the octanucleotide sequence d(GCATATCG).d(CGATATGC). These first solution structures of threaded polypyridyl ruthenium complexes further illustrate that chirality plays an important role in the binding of such complexes to B-DNA. The three stereoisomers display different binding selectivity and kinetics: Λ,Λ-**1** and Δ,Λ-**1** show slow exchange kinetics as they bind to the octanucleotide by threaded intercalation. The Δ,Δ-**1**/DNA complex exists in two bound states in intermediate exchange on the NMR timescale which suggests a dynamic exchange between minor groove binding and intercalation. A comparison between our results and previous studies[6,7,23] suggests that although intercalation into stable duplex DNA is very slow, intercalation is very much faster when the DNA is less stable/more flexible (as in poly-d(AT)) or is destabilized (here, by being very short). An interesting implication is that it may be possible to label DNA opening hotspots such as transcription bubbles, mismatches or abasic sites using suitable ruthenium light switches.

ASSOCIATED CONTENT

Supporting Information. Crystallographic data for the three bis-ruthenium ligands, including experimental methods; CD spectra of Λ,Δ-**1**/DNA complexes; fluorescent lifetime decay curves for the complexes; NOE walk for the free duplex; NMR assignments of the free ligands; table of DNA chemical shifts and shift changes on binding; tables of ligand chemical shifts and shift changes on binding; NOE spectra and lists of intermolecular NOEs; TOCSY spectra of DNA free and bound to Λ,Δ-**1**; EXSY spectra of the Δ,Δ-**1** complex and fits to Arrhenius and Eyring plots; ^{31}P COSY spectra of complexes with Λ,Δ and Λ,Λ-**1**; space-filling views of Λ and Δ stereochemistries in the minor groove. This material is available free of charge via the Internet at http://pubs.acs.org.

AUTHOR INFORMATION

Corresponding Author

*james.thomas@sheffield.ac.uk
*m.williamson@sheffield.ac.uk

ORCID

Jim A. Thomas: 0000-0002-8662-7917

Mike P. Williamson: 0000-0001-5572-1903

Author Contributions

The manuscript was written through contributions of all authors. All authors have given approval to the final version of the manuscript.

Notes

The authors declare no competing financial interests.

ACKNOWLEDGMENTS

FRK and JAT acknowledge the support of The Royal Society and the Royal Society of Chemistry through their "International Exchange Award" and "Journal Grant to International Authors" (respectively) for FRK's sojourn at the University of Sheffield. We thank BBSRC for a White Rose Mechanistic Biology DTP studentship (to SDF).

REFERENCES

(1) Gill, M. R.; Garcia-Lara, J.; Foster, S. J.; Smythe, C.; Battaglia, G.; Thomas, J. A. A ruthenium(II) Polypyridyl Complex for Direct Imaging of DNA Structure in Living Cells. *Nat. Chem.* **2009**, *1* (8), 662–667. https://doi.org/10.1038/nchem.406.

(2) Friedman, A. E.; Chambron, J. C.; Sauvage, J. P.; Turro, N. J.; Barton, J. K. A Molecular Light Switch for DNA: $Ru(bpy)_2(dppz)^{2+}$. *J. Am. Chem. Soc.* **1990**, *112* (12), 4960–4962. https://doi.org/10.1021/ja00168a052.

(3) Wilson, T.; Williamson, M. P.; Thomas, J. A. Differentiating Quadruplexes: Binding Preferences of a Luminescent Dinuclear Ruthenium(II) Complex with Four-Stranded DNA Structures. *Org. Biomol. Chem.* **2010**, *8* (11), 2617–2621. https://doi.org/10.1039/b924263e.

(4) Wilson, T.; Costa, P. J.; Félix, V.; Williamson, M. P.; Thomas, J. A. Structural Studies on Dinuclear Ruthenium(II) Complexes That Bind Diastereoselectively to an Antiparallel Folded Human Telomere Sequence. *J. Med. Chem.* **2013**, *56* (21), 8674–8683. https://doi.org/10.1021/jm401119b.

(5) Wilhelmsson, L. M.; Westerlund, F.; Lincoln, P.; Nordén, B. DNA-Binding of Semirigid Binuclear Ruthenium Complex Δ,Δ-[μ-(11,11′-bidppz)$(phen)_4Ru_2]^{4+}$: Extremely Slow Intercalation Kinetics. *J. Am. Chem. Soc.* **2002**, *124* (41), 12092–12093. https://doi.org/10.1021/ja027252f.

(6) Lutterman, D. A.; Chouai, A.; Liu, Y.; Sun, Y.; Stewart, C. D.; Dunbar, K. R.; Turro, C. Intercalation Is Not Required for DNA Light-Switch Behavior. *J. Am. Chem. Soc.* **2008**, *130* (4), 1163–1170. https://doi.org/10.1021/ja071001v.

(7) Andersson, J.; Li, M.; Lincoln, P. AT-Specific DNA Binding of Binuclear Ruthenium Complexes at the Border of Threading Intercalation. *Chem. - A Eur. J.* **2010**, *16* (36), 11037–11046. https://doi.org/10.1002/chem.201000180.

(8) Wilhelmsson, L. M.; Esborner, E. K.; Westerlund, F.; Nordén, B.; Lincoln, P. Meso Stereoisomer as a Probe of Enantioselective Threading Intercalation of Semirigid Ruthenium Complex $[\mu\text{-}(11,11'\text{-bidppz})(phen)_4Ru_2]^{4+}$. *J. Phys. Chem. B* **2003**, *107* (42), 11784–11793. https://doi.org/10.1021/jp036302f.

(9) Önfelt, B.; Lincoln, P.; Nordén, B. Enantioselective DNA Threading Dynamics by Phenazine-Linked $[Ru(phen)_2dppz]^{2+}$ Dimers. *J. Am. Chem. Soc.* **2001**, *123* (16), 3630–3637. https://doi.org/10.1021/ja003624d.

(10) Waywell, P.; Thomas, J. A.; Williamson, M. P. Structural Analysis of the Binding of the Diquaternary Pyridophenazine Derivative dqdppn to B-DNA Oligonucleotides. *Org. Biomol. Chem.* **2010**, *8* (3), 648–654. https://doi.org/10.1039/b918252g.

(11) Bolger, J.; Gourdon, A.; Ishow, E.; Launay, J.-P. Mononuclear and Binuclear Tetrapyrido[3,2- a□:2‘,3‘-c□:3‘‘,2‘‘- H□:2‘‘‘,3‘‘‘- J]Phenazine (tpphz) Ruthenium and Osmium Complexes. *Inorg. Chem.* **1996**, *35* (10), 2937–2944. https://doi.org/10.1021/ic951436w.

(12) Brünger, A. T.; Adams, P. D.; Clore, G. M.; Delano, W. L.; Gros, P.; Grossekunstleve, R. W.; Jiang, J. S.;

Kuszewski, J.; Nilges, M.; Pannu, N. S.; et al. Crystallography & NMR System: A New Software Suite for Macromolecular Structure Determination. *Acta Crystallogr. Sect. D Biol. Crystallogr.* **1998**, *54* (5), 905–921. https://doi.org/10.1107/S0907444998003254.

(13) Brunger, A. T. Version 1.2 of the Crystallography and Nmr System. *Nat. Protoc.* **2007**, *2* (11), 2728–2733. https://doi.org/10.1038/nprot.2007.406.

(14) Kleywegt, G. J. Dictionaries for Heteros. *Newsl. Protein Crystallograpy* **1995**, *31*, 45–50.

(15) Arnott, S.; Campbell-smith, P. J.; Chandrasekaran, R. *In Handbook of Biochemistry and Molecular Biology*, 3rd ed.; Fasman, G. P., Ed.; CRC Press: Cleveland, 1976.

(16) Lee, J.; Guelev, V.; Sorey, S.; Hoffman, D. W.; Iverson, B. L. NMR Structural Analysis of a Modular Threading Tetraintercalator Bound to DNA. *J. Am. Chem. Soc.* **2004**, *126* (43), 14036–14042. https://doi.org/10.1021/ja046335o.

(17) Neuhaus, D.; Williamson, M. *The Nuclear Overhauser Effect in Structural and Conformational Analysis*; 2000.

(18) Richard Keene, F. Isolation and Characterisation of Stereoisomers in Di- And Tri-Nuclear Complexes. *Chem. Soc. Rev.* **1998**, *27* (3), 185–193. https://doi.org/10.1039/a827185z.

(19) Fletcher, N. C.; Junk, P. C.; Reitsma, D. A.; Keene, F. R. Chromatographic Separation of Stereoisomers of Ligand-Bridged Diruthenium Polypyridyl Species. *J. Chem. Soc. Dalt. Trans.* **1998** (1), 133–138. https://doi.org/10.1039/a705947g.

(20) Andersson, J.; Lincoln, P. Stereoselectivity for DNA Threading Intercalation of Short Binuclear Ruthenium Complexes. *J. Phys. Chem. B* **2011**, *115* (49), 14768–14775. https://doi.org/10.1021/jp2062767.

(21) Bolger, J.; Gourdon, A.; Ishow, E.; Launay, J.-P. Stepwise Syntheses of Mono- and Di-Nuclear Ruthenium tpphz Complexes $[(Bpy)_2Ru(tpphz)]_2$– and $[(Bpy)_2Ru(tpphz)Ru(bpy)_2]^{4+}$ {tpphz = tetrapyrido[3,2-a: 2′,3′-c: 3″,2″-H: 2″,3□-J]phenazine}. *J. Chem. Soc., Chem. Commun.* **1995** (17), 1799–1800. https://doi.org/10.1039/C39950001799.

(22) Foley, F. M.; Keene, F. R.; Collins, J. G. The DNA Binding of the ΔΔ-, ΔΛ- and ΛΛ-Stereoisomers of $[\{Ru(Me_2bpy)_2\}_2(\mu\text{-bpm})]^{4+}$. *J. Chem. Soc. Dalt. Trans.* **2001** (20), 2968. https://doi.org/10.1039/b103368a.

(23) Scheeck, R. M.; Boelens, R.; Russo, N.; Van Boom, J. H.; Kaptein, R. Sequential Resonance Assignments in H NMR Spectra of Oligonucleotides by Two-Dimensional NMR Spectroscopy. *Biochemistry* **1984**, *23* (7), 1371–1376.

(24) Patel, D. J.; Shapiro, L.; Hare, D. Sequence-Dependent Conformation of DNA Duplexes. The AATT Segment of the d(G-G-A-A-T-T-C-C) Duplex in Aqueous Solution. *J. Biol. Chem.* **1986**, *261* (3), 1223–1229.

(25) Dupureur, C. M.; Barton, J. K. Use of Selective Deuteration and ^{1}H NMR in Demonstrating Major Groove Binding of Δ-$[Ru(phen)_2dppz]^{2+}$ to $d(GTCGAC)_2$. *J. Am. Chem. Soc.* **1994**, *116* (22), 10286–10287. https://doi.org/10.1021/ja00101a053.

(26) Nordell, P.; Westerlund, F.; Wilhelmsson, L. M.; Nordén, B.; Lincoln, P. Kinetic Recognition of AT-Rich DNA by Ruthenium Complexes. *Angew. Chemie Int. Ed.* **2007**, *46* (13), 2203–2206. https://doi.org/10.1002/anie.200604294.

(27) Packer, M. J.; Dauncey, M. P.; Hunter, C. A. Sequence-Dependent DNA Structure: Dinucleotide Conformational Maps. *J. Mol. Biol.* **2000**, *295* (1), 71–83. https://doi.org/10.1006/jmbi.1999.3236.

(28) Wu, L.; Reymer, A.; Persson, C.; Kazimierczuk, K.; Brown, T.; Lincoln, P.; Nordén, B.; Billeter, M. Initial DNA Interactions of the Binuclear Threading Intercalator Λ,Λ-$[\mu\text{-Bidppz}(bipy)_4Ru_2]^{4+}$□: An NMR Study with $[d(CGCGAATTCGCG)]_2$. *Chem. Eur. J.* **2013**, *19* (17), 5401–5410. https://doi.org/10.1002/chem.201203175.

(29) Zimmer, K. D.; Shoemaker, R.; Ruminski, R. R. Synthesis and Characterization of a Fluxional Re(I) Carbonyl Complex Fac-$[Re(CO)_3(dpop')Cl]$ with the Nominally Tri-Dentate Ligand dipyrido(2,3-a:3′,2′-J)phenazine (Dpop′). *Inorganica Chim. Acta* **2006**, *359* (5), 1478–1484. https://doi.org/10.1016/j.ica.2005.11.042.

(30) Hall, J. P.; Cook, D.; Morte, S. R.; McIntyre, P.; Buchner, K.; Beer, H.; Cardin, D. J.; Brazier, J. A.; Winter, G.; Kelly, J. M.; et al. X-Ray Crystal Structure of Rac-$[Ru(phen)_2dppz]^{2+}$ with $d(ATGCAT)_2$ Shows Enantiomer Orientations and Water Ordering. *J. Am. Chem. Soc.* **2013**, *135* (34), 12652–12659. https://doi.org/10.1021/ja403590e.

(31) Hall, J. P.; Keane, P. M.; Beer, H.; Buchner, K.; Winter, G.; Sorensen, T. L.; Cardin, D. J.; Brazier, J. A.; Cardin, C. J. Delta Chirality Ruthenium "Light-Switch" Complexes Can Bind in the Minor Groove of DNA with Five Different Binding Modes. *Nucleic Acids Res.* **2016**, *44* (19), 9472–9482. https://doi.org/10.1093/nar/gkw753.

(32) Song, H.; Kaiser, J. T.; Barton, J. K. Crystal Structure of Δ-$[Ru(bpy)$□$dppz]^{2+}$ Bound to Mismatched DNA Reveals Side-by-Side Metalloinsertion and Intercalation. *Nat. Chem.* **2012**, *4* (8), 615–620. https://doi.org/10.1038/nchem.1375.

(33) Goldfield, E. M.; Luxon, B. A.; Bowie, V.; Gorenstein, D. G. Phosphorus-31 Nuclear Magnetic Resonance of Ethidium Complexes with Ribonucleic Acid Model Systems and Phenylalanine-Accepting Transfer Ribonucleic Acid1" *Biochemistry* **1983**, *22*, 3336–3344.